Title

CD14+CD16+ monocytes are the main target of Zika virus infection in peripheral blood mononuclear cells in a paediatric study in Nicaragua

Journal

Nature Microbiology, 2(11)

ISSN

2058-5276

Authors

Michlmayr, Daniela
Andrade, Paulina
Gonzalez, Karla
et al.

Publication Date

2017-11-01

DOI

10.1038/s41564-017-0035-0

Peer reviewed

HHS Public Access

Author manuscript

Nat Microbiol. Author manuscript; available in PMC 2018 June 12.

Published in final edited form as:

Nat Microbiol. 2017 November ; 2(11): 1462–1470. doi:10.1038/s41564-017-0035-0.

$CD14^+CD16^+$ monocytes are the main target of Zika virus infection in peripheral blood mononuclear cells in a paediatric study in Nicaragua

Daniela Michlmayr[1], **Paulina Andrade**[1,2], **Karla Gonzalez**[3,4], **Angel Balmaseda**[3,4], and **Eva Harris**[1,*]

[1]Division of Infectious Diseases and Vaccinology, School of Public Health, University of California, Berkeley, Berkeley 94720-3370 CA, USA

[2]Universidad de San Francisco de Quito, Quito 170157, Ecuador

[3]Sustainable Sciences Institute, Managua 14007, Nicaragua

[4]Laboratorio Nacional de Virología, Centro Nacional de Diagnóstico y Referencia, Ministry of Health, Managua 16064, Nicaragua

Abstract

The recent Zika pandemic in the Americas is linked to congenital birth defects and Guillain-Barré syndrome. White blood cells (WBCs) play an important role in host immune responses early in arboviral infection. Infected WBCs can also function as 'Trojan horses' and carry viruses into immune-sheltered spaces, including the placenta, testes and brain. Therefore, defining which WBCs are permissive to Zika virus (ZIKV) is critical. Here, we analyse ZIKV infectivity of peripheral blood mononuclear cells (PBMCs) in vitro and from Nicaraguan Zika patients and show $CD14^+CD16^+$ monocytes are the main target of infection, with ZIKV replication detected in some dendritic cells. The frequency of $CD14^+$ monocytes was significantly decreased, while the $CD14^+CD16^+$ monocyte population was significantly expanded during ZIKV infection compared to uninfected controls. Viral RNA was detected in PBMCs from all patients, but in serum from only a subset, suggesting PBMCs may be a reservoir for ZIKV. In Zika patients, the frequency of infected cells was lower but the percentage of infected $CD14^+CD16^+$ monocytes was significantly higher compared to dengue cases. The gene expression profile in monocytes isolated from ZIKV- and dengue virus-infected patients was comparable, except for significant differences in interferon-γ, CXCL12, XCL1, interleukin-6 and interleukin-10 levels. Thus, our study provides a

[*]**Correspondence and requests for materials** should be addressed to E.H. eharris@berkeley.edu.

Author contributions

D.M., P.A. and E.H. conceived and designed the experiments. D.M, P.A. and K.G. performed experiments. D.M., P.A. and E.H. analysed the data. A.B. and E.H. directed the human studies. D.M., P.A. and E.H. wrote the manuscript. All authors reviewed the manuscript.

Competing interests

The authors declare no competing financial interests.

Supplementary information is available for this paper at https://doi.org/10.1038/s41564-017-0035-0.

detailed picture of the innate immune profile of ZIKV infection and highlights the important role of monocytes, and $CD14^+CD16^+$ monocytes in particular.

Zika virus (ZIKV) is an arthropod-borne positive-sense RNA flavivirus, composed of seven non-structural and three structural proteins[1]. Since 2015, ZIKV has spread rapidly throughout the Americas, concurrent with an increase in congenital birth defects, including microcephaly and Guillain–Barré syndrome[2]. ZIKV infection can be asymptomatic or can cause a mild febrile illness clinically resembling infection with other co-circulating arboviruses, including dengue (DENV) and chikungunya (CHIKV) viruses. At present, it is unclear how ZIKV reaches immune-privileged sites within the body and breaches protective placental-fetal and blood-testis barriers, which leads to sexual transmission and congenital defects[3]. One possible route is ZIKV-infected white blood cells (WBCs), which disseminate the virus into different compartments of the body or serve as a viral reservoir upon recruitment to the infection site, a mechanism known as 'Trojan horse'[4]. West Nile virus (WNV), another flavivirus, infects monocytes, contributing to its dissemination into the brain, resulting in encephalitis and meningitis[5,6]. Monocytes and dendritic cells (DCs) are the main target of DENV infection in human peripheral blood mononuclear cells (PBMCs) and in the skin[7–9].

Here, we identify cellular targets of ZIKV in human blood, compare this to DENV-infected patients, and analyse gene expression profiles of monocytes isolated from ZIKV- and DENV-infected patients. Our results reveal a detailed immune profile of ZIKV infection in PBMCs in vitro and in patients, which is pivotal to understanding the initial stages of Zika pathogenesis prior to dissemination throughout the body and into immune-sheltered sites, leading to neurological complications and vertical and sexual transmission of the virus.

To determine whether WBCs become infected with ZIKV, we first infected isolated PBMCs from four healthy blood donors for 48 h and stained intracellularly for ZIKV E and NS3 proteins to identify replicating virus. Immunophenotyping of in-vitro-infected cells showed a significantly higher percentage and number of $CD14^+CD16^+$ monocytes ($P < 0.01$), a significantly lower percentage and number of $CD14^+$ monocytes ($P < 0.01$ and $P < 0.05$, respectively) and a lower percentage of $CD16^+$ monocytes ($P < 0.05$) compared to uninfected PBMCs (Fig. 1a-c). In addition, the $CD14^+CD16^+$ monocyte population increased, while $CD14^+$ monocytes decreased from 24 h to 48 h post-infection (Supplementary Fig. 1a). The mean percentage of B cells was somewhat increased ($P < 0.05$), $CD4^+$ memory T cells decreased ($P < 0.01$), and myeloid (mDC) and plasmacytoid (pDC) DCs, NK cells, $CD8^+$ T cells, and naive and effector $CD4^+$ T cells remained the same compared to uninfected cells (Fig. 1d-f and Supplementary Fig. 1c-j). We found that an average of 6.8% of all live PBMCs were actively infected in vitro, consisting of 83.7% monocytes, 14.8% mDCs, 1.1% B cells, 0.1% T cells and 0.7% NK cells (Fig. 1g,h). Among monocytic cells, 58.3% of all monocytes were infected, with $CD14^+CD16^+$ monocytes being the main target of ZIKV at 48 h post-infection, followed by $CD14^+$ monocytes (Fig. 1i,j). Within DCs, mDCs were infected while pDCs were not (Fig. 1k and Supplementary Fig. 2a), and more $CD8^+$ T cells than $CD4^+$ T cells were infected; however, ZIKV-infected T cells were found at very low frequency (Fig. 1l and Supplementary Fig. 2b), similar to NK

and B cells (Supplementary Fig. 2c-e). Thus, PBMCs are susceptible to ZIKV infection in vitro, with monocytes being the main target.

We then analysed PBMCs collected during acute illness from 29 ZIKV-infected and 8 DENV-infected patients enrolled in a paediatric hospital study in Managua, Nicaragua (Supplementary Table 1). To more accurately compare the clinical characteristics of Zika and dengue patients, Zika cases were stratified into earlier (1-2) and later (3-6) days of illness at enrolment, and the latter compared to dengue cases (3-6 days). Of the Zika and dengue patients, 63.2% and 37.5% had been exposed to DENV previously. Almost all (94.7%) Zika, compared to 50% of dengue cases, respectively, developed rash ($P < 0.01$). Conjunctivitis, arthralgia and abdominal pain were not significantly different. All dengue cases were febrile at enrolment, whereas Zika cases were not ($P < 0.0001$). In Zika patients, the frequency of WBCs and monocytes did not change over the three days of hospitalization corresponding to the first six days post-illness (Supplementary Fig. 3a,b). However, almost half the Zika patients had monocytosis, whereas the monocyte count in dengue patients was normal (Supplementary Fig. 3b). Monocytosis is important for the rapid control of virus and clearance from the body and is associated with reduced viral titres in the central nervous system (CNS) and lower mortality in mice[4,10,11].

ZIKV RNA was measured in serum and urine by real-time reverse transcription-polymerase chain reaction (RT-PCR) on day 1 of presentation, corresponding to days 1 to 6 of illness. All patients were negative for DENV and CHIKV. ZIKV was detectable exclusively in serum in 6 patients (21%), whereas 9 (31%) and 14 (48%) patients were ZIKV-positive in serum and urine or were serum-negative but urine-positive, respectively (Fig. 2a,b)[2,12]. ZIKV in serum and PBMCs was quantified by quantitative reverse transcription-polymerase chain reaction (qRT-PCR) on days 1-3 post-presentation; viraemia peaked on days 1-3 post-onset of symptoms and declined thereafter, whereas no significant differences in viral load were detected in PBMCs at days 1–6 post-symptom onset (Fig. 2b,c). Thus, ZIKV RNA is detectable in PBMCs longer than in serum, suggesting that WBCs may function as a potential reservoir. Similarly, PBMCs are permissive to infection with DENV and WNV[1,3,6–8]. However, the level of ZIKV infection in PBMCs was lower than in serum, suggesting that other sources may contribute to viraemia.

Based on phenotypic differences detected in vitro, we next determined the impact of ZIKV infection in the WBCs of Zika patients. For each patient, we analysed PBMCs collected on days 1, 2 and 3 post-presentation and did not detect differences in any cell populations over time (Supplementary Fig. 3c–i). Thereafter, we selected day 1 post-enrolment for phenotypic cell comparisons to healthy uninfected blood donors (Fig. 2d–h). The overall proportions of cell populations within each patient were comparable to healthy individuals (Supplementary Fig. 4a,b). To identify changes within monocytes, we first gated cells on $CD11b^{+}HLA\text{-}DR^{+}$ and examined the level of CD14 and CD16 expression (Fig. 2d,e). ZIKV infection resulted in significant expansion of $CD14^{+}CD16^{+}$ monocytes compared to uninfected individuals ($P < 0.01$), although the overall frequency and absolute cell number was low in all patient samples, and there was a reduction in the percentage and number of classical ($CD14^{+}CD16^{-}$) monocytes ($P < 0.05$) (Fig. 2e and Supplementary Fig. 4c). Thus, we found $CD14^{+}CD16^{+}$ monocytes are expanded during ZIKV infection in vitro and in vivo,

consistent with other studies of HIV or DENV infection[2,4,13,14]. $CD14^+CD16^+$ monocytes produce large quantities of inflammatory cytokines and display high phagocytic activity, contributing to an inflammatory immune response to clear pathogens[1,5,6,14]. $CD14^+CD16^+$ monocytes can quickly differentiate into DCs and activate T cells during viral infection[2,7–9,15], as well as induce plasmablast differentiation and antibody responses during acute DENV infection in humans and primates, demonstrating they are important mediators of adaptive immune responses[3,5,7,13]. Therefore, $CD14^+CD16^+$ monocytes may play an important role in the immune response during ZIKV infection, and additional studies are needed to determine the exact role of monocytes during ZIKV pathogenesis.

Next, we gated WBCs on $CD3^+$ T cells and found an increase in the percentage of $CD4^+$ T cells ($P < 0.05$) and naive $CD4^+$ T cells ($P < 0.001$) and a decrease in $CD8^+$ T cells ($P < 0.05$), $CD4^+$ effector memory T cells ($P < 0.001$) and $CD4^+$ effector T cells compared to healthy individuals (Fig. 2f-h and Supplementary Fig. 4d). The percentage of pDCs was higher in ZIKV-infected patients ($P < 0.05$) (Supplementary Fig. 4e), while mDCs, NK cells and B cells were unchanged (Supplemental Fig. 4f-h).

We then examined which WBCs are targeted by ZIKV during acute infection by staining a subset ($n = 19$) of the same patients from the phenotypic analysis (Fig. 2) with antibodies against E and NS3 protein. As the viral titre in PBMCs was similar across days 1-6 of illness (Fig. 2c), we analysed all patient samples from day 1 of presentation, which corresponds to a mean of 3.3 days of illness. After gating WBCs from ZIKV-infected patients on E- and NS3-double-positive cells we found that an average of 4.6% of all PBMCs become infected. While many studies of ZIKV exclusively use anti-E antibodies, our study demonstrates that both antibodies are necessary to identify ZIKV-infected cells, as 32-40% of the E staining was detected on the surface of in-vitro-infected cells and PBMCs from Zika patients and does not necessarily imply infection (Supplementary Fig. 5; see Methods). Within the patients' infected (E^+NS3^+) WBCs, 82.6% were monocytes, 10.7% mDCs, 2% NK cells, 0.8% B cells and 0.6% T cells (Fig. 3a). Furthermore, of all E^+NS3^+ WBCs, a mean of 18.8 ± 11.3% (s.d.) were $CD14^+$, 59.8 ± 16.1% were $CD14^+CD16^+$ and 4 ± 3.5% were $CD16^+$ monocytes (Fig. 3b). Thus, $CD14^+CD16^+$ monocytes are the main target of infection within WBCs of patients, consistent with our in vitro experiments.

Studies of WNV and DENV infection in humans have also shown monocytes and macrophages to be highly susceptible to infection[5–7]. Several receptors, including DC-SIGN, AXL, Tyro 3 and TIM-1, have been described as possible entry receptors for ZIKV into cells. In particular, the TAM receptor AXL has been identified as an entry factor for ZIKV in fetal endothelial, microglia and other brain cells[16–18]. Interestingly, AXL and the other receptors are also strongly expressed on monocytes, macrophages and DCs, all of which are highly susceptible to ZIKV infection[19]. The closely related DENV uses AXL for entry into cells through indirect binding to AXL via Gas6[20]. Therefore, we speculate that AXL could also play a role in ZIKV infection of monocytes; however, further studies are needed to determine the role of AXL and other receptors, such as DC-SIGN and Tyro3, in the tropism of ZIKV for monocyte populations.

Monocytes can play a pathogenic role upon infection by flaviviruses and other pathogens by contributing to the spread of infection within the body via the 'Trojan horse' mechanism, whereby monocytes infected directly or indirectly disseminate virus and thereby potentiate disease and increase mortality[7–9,15,21]. In animal models of HIV and WNV infection, virus is spread into the CNS through infiltration of infected monocytes across the blood-brain barrier[4,10,22–24]. HIV-infected monocytes and T cells can also disseminate infection across the blood-testis barrier, resulting in sexual transmission of HIV through infected sperm[2,25,26]. Because ZIKV is also sexually transmitted through infected sperm, infected WBCs could be a vehicle for transporting virus across the blood-testis barrier[3,6–8,27].

We found that mDCs are also susceptible to ZIKV infection, but that the percentage of pDCs in blood is increased during ZIKV infection. pDCs are major producers of type I interferon after viral exposure[13,14,28,29], and their increase results in reduced disease severity[30]. Thus, the observed increase of pDCs during ZIKV infection could have beneficial implications for Zika pathogenesis.

ZIKV is closely related to the flavivirus DENV, so we compared the immune profile of ZIKV to DENV infection by analysing samples from day 1 post-enrolment from dengue patients in the same hospital-based study. We found that DENV infects 4.5-fold more PBMCs than ZIKV ($P < 0.0001$, Fig. 3c,d). The percentage of classical $CD14^+$ monocytes was higher ($P < 0.01$) and that of $CD16^+$ monocytes was decreased in ZIKV-compared to DENV-infected patients ($P < 0.001$) (Fig. 3e and Supplementary Fig. 6a), while the percentage of $CD14^+CD16^+$ monocytes was similar in both groups. However, $CD14^+CD16^+$ monocytes were significantly more infected with ZIKV compared to DENV ($P < 0.01$), while infection of $CD16^+$ monocytes was higher in DENV-infected compared to ZIKV-infected patients ($P < 0.05$) (Fig. 3f). Similarly, the frequency of $CD4^+$ T cells was elevated, whereas $CD8^+$ T cells were decreased during ZIKV infection compared to DENV ($P < 0.01$) (Fig. 3g and Supplementary Fig. 6b), and significantly fewer $CD3^+$ T cells became infected in Zika patients ($P < 0.01$) (Fig. 3h and Supplementary Fig. 6c). The frequency of NK cells was significantly reduced in Zika cases ($P < 0.001$) (Fig. 3i and Supplementary Fig. 6d), while mDC and B cell frequency was not different (Supplementary Fig. 6e,f). Thus, WBCs from patients are less susceptible to ZIKV infection compared to DENV, and phenotypic differences occur between ZIKV- and DENV-infected patients, despite the close structural similarity of the viruses.

Next, we analysed the transcriptional profile of monocytes infected in vitro with ZIKV for 24 and 48 h compared to monocytes from healthy uninfected blood donors using a TaqMan gene expression assay. Certain chemokines were > 1,000-fold or 100-700-fold upregulated (Fig. 4a), including several chemokines (for example, CXCL8[31]) important for neutrophil trafficking. Neutrophils could play a critical role in ZIKV pathogenesis or control; studies with WNV and Japanese encephalitis virus have demonstrated that neutrophils serve as a virus reservoir and facilitate viral dissemination[32,33]. Interestingly, many genes involved in the immune response and almost all interleukins were not differentially expressed during ZIKV infection.

Finally, we compared the gene expression profile of monocytes in ZIKV-versus DENV-infected patients and found a similar profile, with many genes upregulated and four genes downregulated during both infections (Fig. 4b, Supplementary Fig. 7 and Supplementary Table 2). Genes that were > 100-fold upregulated during ZIKV or DENV infection were CCL2, CXCL12, XCL1, CXCR5, IL-6, PF4/CXCL4 and IFN-γ (Supplementary Fig. 7 and Supplementary Table 2). The median expression of CXCL12 and IL-6 was > 100-fold higher during ZIKV infection ($P < 0.05$), while expression of XCL1, interferon (IFN)-γ and interleukin (IL)-10 was >100-fold higher during DENV infection ($P < 0.05$) (Fig. 4b and Supplementary Fig. 7). Thus, the cytokine expression profile induced in monocytes in the blood of ZIKV- and DENV-infected patients is comparable but differs in selected inflammatory cytokines. Chemokines with an important role in the chemotactic activity of monocytes and T cells were upregulated in both diseases. However, CXCL12 was significantly higher in monocytes during ZIKV infection. Dysregulation of CXCL12 is associated with reduced integrity of the blood-brain barrier during viral encephalitis[34,35]. WNV studies showed that CXCL12 is implicated in WBC retention in the CNS perivascular space and regulation of $CD8^+$ T cell trafficking into the brain for viral clearance[36]. Thus, CXCL12 could play a role in inflammation of the brain in the fetus and associated brain abnormalities.

In summary, we have shown that WBCs are permissive to ZIKV infection and that monocytes, particularly $CD14^+CD16^+$ monocytes, followed by DCs, are the main target of infection. Because monocytes can infiltrate many tissues, including immune-sheltered organs, they are ideal targets for infection, as they can act as ‘Trojan horses’. We found that the percentage of $CD14^+CD16^+$ monocytes is increased, consistent with their role in infection with DENV[13]. The gene expression profile of monocytes during ZIKV infection is generally muted, with low induction of cytokines/chemokines, consistent with the mild symptomatology of Zika. Identifying cellular targets of ZIKV infection in the blood is an important step in understanding the early stages of the ZIKV-induced innate immune response, when drug therapies could be applied to prevent complications and severe outcomes of Zika. Future studies are needed to define the specific role monocytes play during ZIKV pathogenesis and how they contribute to dissemination via the maternal-fetal and blood–testis barriers.

Methods

Study design and population

PBMCs from ZIKV-infected patients were obtained from an ongoing study in the Infectious Disease Ward of the Nicaraguan National Pediatric Reference Hospital, Hospital Infantil Manuel de Jesús Rivera (HIMJR), in Managua, Nicaragua, between July and August of 2016. PBMCs from dengue patients were obtained between July and August of 2016 and between September and November of 2012. Suspected Zika and dengue cases presenting to the HIMJR 1-6 days post-symptom onset were enrolled after informed consent, and blood and urine were collected on days 1, 2 and 3 post-enrolment. Children were examined by study physicians, and clinical data were recorded systematically on study collection forms. Enrolment criteria consisted of age less than 15 years and presentation with an acute febrile

illness of fewer than 7 days duration consistent with the case definition for dengue or Zika (the latter, rash with one or more of the following symptoms: conjunctivitis, arthralgia, myalgia and/or periarticular oedema regardless of fever)[37]. ZIKV and DENV infection were confirmed by real-time RT-PCR performed at the National Virology Laboratory of the Ministry of Health in Managua using either of two triplex assays that simultaneously detect ZIKV, CHIKV and DENV infections: the ZCD assay[38] or the CDC Trioplex assay[39]. Patients with acute ZIKV infection (n = 29) or DENV infection (n = 3 DENV2 from 2016 and $n = 5$ DENV1 from 2012) were selected for our study. For the comparison of PBMCs from Zika versus dengue, Zika and dengue patients presenting to the hospital on days 3-6 of illness (mean 3.8 (±0.9) for Zika and mean 4.5 (±1.1) days for dengue, $P > 0.05$) were included in the analysis. The hospital study was reviewed and approved by the Institutional Review Boards (IRB) of the University of California, Berkeley, and the Nicaraguan Ministry of Health. Parents or legal guardians of all subjects provided written informed consent, and subjects 6 years of age and older provided assent. Healthy blood donor samples were collected at the American Red Cross Blood Donation Center and the Nicaraguan National Blood Bank, with two adult patient samples from Oakland and four adult patient samples from Nicaragua, respectively.

PBMC isolation

Daily blood samples were collected on days 1, 2 and 3 post-enrolment into the hospital study. PBMCs, plasma and serum were prepared as previously described[7,40]. For PBMC preparation, blood samples were collected in Vacutainer tubes (Becton-Dickenson) with EDTA anticoagulant reagent. Upon receipt in the Nicaraguan National Virology Laboratory, 4-5 ml of blood was transferred into a Leucosep tube (Greiner Bio-One) containing 3 ml of Ficoll Histopaque (Sigma) and centrifuged at 500*g* for 20 min at room temperature. The PBMC fraction was collected and transferred to a 15 ml conical tube containing 9 ml of PBS with 2% fetal bovine serum (FBS; Denville Scientific) and 1% penicillin/streptomycin (Sigma). Cells were washed three times in this solution by centrifugation at 500*g* for 10 min and resuspended in 10 ml of complete medium. Before the third wash, an aliquot was used to obtain a cell count using a haematology analyser (Sismex XS-1000i). After the third wash, cells were resuspended at a concentration of 10^7 cells per ml in freezing medium consisting of 90% FBS and 10% dimethyl sulfoxide, and aliquoted. Cryovials containing the cell suspension were placed in isopropanol containers (Mr. Frosty, Nalgene) at −80 °C overnight and transferred to liquid nitrogen for storage. For in vitro infection experiments, PBMCs were isolated from Buffy coats from healthy blood donors obtained from the American Red Cross Oakland Blood Donation Center and the Nicaraguan National Blood Bank using the protocol described above.

Monocyte isolation

Monocytes were isolated from PBMCs of healthy blood donors and from ZIKV- and DENV-infected patients from the Nicaraguan hospital study using the Pan-monocyte Isolation Kit (Miltenyi) according to the manufacturer's protocol. In brief, PBMCs were quickly thawed at 37 °C and washed twice in RPMI containing 10% FBS, 2 mM L-glutamine and 1% penicillin/streptomycin. The cells were then blocked with 10 μl FcR-blocking reagent and stained with 10 μl biotin-antibody cocktail for 5 min at 4 °C. After incubation, cells were

stained with 20 μl anti-biotin Microbeads (Miltenyi) for 10 min at 4 °C. For manual separation, an LS cell separation column (Miltenyi) was placed into a MACS Separator (Miltenyi), and the negative fraction containing the flow-through of enriched and unlabelled monocytes was collected and counted. The purity of the isolated monocyte populations was determined by flow cytometry using the markers CD11b, CD14 and CD16, and was found to be >95% pure.

Virus and in vitro infection of PBMCs and monocytes

ZIKV strain Nica 2-16 was used for in vitro experiments and was initially isolated in early 2016 from a ZIKV-infected patient by the National Virology Laboratory, Nicaraguan Ministry of Health[41]. Nica 2–16 was propagated at low passage in C6/36 cells in MEM (Gibco) supplemented with 5% FBS, 1% penicillin/streptomycin, and 2 mM L-glutamine (Invitrogen), and cell-free supernatants were collected 4, 5 and 6 days post-infection (p.i.). The C6/36 cells were donated by R. Baric, University of North Carolina, Chapel Hill. Cells were tested for DENV and ZIKV contamination by RT-PCR and for mycoplasma contamination by PCR. This cell line is not listed in the database of commonly misidentified cell lines maintained by ICLAC and NCBI Biosample. For in vitro infections, PBMCs from healthy blood donors were plated onto a 24-well plate (Corning), and 2 to 5×10^5 cells per well were infected with Nica 2–16 at a multiplicity of infection (MOI) of 1 for 1 h in serum-free RPMI at 37 °C. Fresh medium was then added to each well, and PBMCs were collected at 48 h and 72 h p.i. for analysis by flow cytometry and immunofluorescence. Isolated monocytes were infected with Nica 2-16 for 1 h at 37 °C in serum-free DMEM medium before adding DMEM supplemented with 5% FBS and 1% penicillin/streptomycin. Monocytes were isolated after 24 and 48 h of infection in vitro and from infected patients, and cell pellets were resuspended in 1 ml of Trizol for RNA extraction and subsequent TaqMan gene expression analysis.

Flow cytometry

PBMCs were removed from liquid nitrogen storage and quickly thawed at 37 °C. Thawed cells were then washed with RPMI (Gibco) supplemented with 10% FBS, 2 mM L-glutamine and 1% penicillin/streptomycin and centrifuged for 5 min at 300g before counting cells with a haemocytometer. PBMCs were then resuspended in flow cytometry buffer (PBS without Ca^{2+}/Mg^{2+} containing 2% FBS and 2 mM EDTA (LifeTech)) and stained with 1:100 Zombie Aqua (BioLegend) viability dye for 15 min at room temperature. PBMCs were divided into different wells of a 96-well plate, distributing between 70,000 and 200,000 cells per well. Next, PBMCs were blocked with human Fc block (1:100, Miltenyi) for 10 min at 4 °C, and the appropriate antibody cocktail for each staining panel was added to each sample and stained for 20 min at 4 °C for surface markers. All antibodies were obtained from eBioscience unless stated otherwise: CD45RA, CD45RO, CD3, CD4, CD8, CCR7, CD11b, CD16, CD14, CCR2, CD1a, CD1c, CD209, CD11c, CD56, CD27, IgM, CD19, CD38, CD20, CD123 and HLA-DR. For data acquisition, the samples were read with an LSR Fortessa high-throughput sampler (HTS) plate reader (BD Biosciences) with 405, 488, 562 and 632 nm laser excitation lines and were analysed using FlowJo software (TreeStar) version 10.2. All cells were gated on live WBCs that were negative for Zombie Aqua dye. Negative and positive gates were determined using isotype controls, uninfected controls

and/or ‘Fluorescence Minus One’ controls. A doublet-exclusion using SSC-Area versus SSC-Height was performed for all samples. To set up a compensation matrix, BD CompBeads (BD Biosciences) were used.

Staining for viral proteins by flow cytometry

To identify ZIKV- and DENV-infected cells, a Cytofix/Cytperm kit (BD) was used for intracellular staining with a pan-flavivirus mAb against the envelope protein, E (4G2, ATCC) and a mAb against nonstructural protein 3, NS3 (E1D8[42]) as per the manufacturer’s protocol. To remove bound virus from the cell surface, cells were incubated with trypsin for 60 min on ice and washed with flow cytometry buffer prior to performing intracellular staining. mAbs 4G2 and E1D8 were conjugated with phycoerythrin (PE) and Alexa Fluor 647, respectively, using protein-labelling kits (Thermo Fisher), and were used at a concentration of 1:500 to 1:800. For isotype controls for 4G2 and E1D8, a mouse IgG2a and mouse IgG2b were used, respectively. To assess the proportion of actively infected cells among E^+-positive cells, because staining for E alone is widely used in the field, we stained with only 4G2 and found that an average of 9.1% (±2.4 s.d.) of WBCs were positive for ZIKV E in in-vitro-infected PBMCs and 8.4% (±2.6 s.d.) were ZIKV E^+ in patient samples (n = 29, Supplementary Fig. 5). When we also stained for NS3 protein, which is expressed only by replicating virus, we found that an average of 6.8% (±0.9) and 4.6% (±1.7) of WBCs were double-positive for E and NS3 in in-vitro-infected cells and Zika patients (n = 19), respectively (Supplementary Fig. 5). To determine how much virus is adherent on the surface of cells, we tested non-permeabilized PBMCs from the same cells and patients and performed surface staining with mAbs against E and NS3. We found that 2.7% (±1.2) and 3.4% (±0.9) of in-vitro-infected cells and patient PBMCs were positive for E on the cell surface, respectively (Supplementary Fig. 5), whereas no NS3 was detectable on the surface of cells. Together, these results indicate that 68-60% of the E protein detected by intracellular and surface staining is from replicating virus and the other 32-40% adheres to the surface of cells, while only a minimal amount of virus is phagocytosed. Thus, to determine the frequency of replicating ZIKV, it is necessary to use the E and NS3 antibodies in conjunction.

RNA extraction and qRT-PCR

To quantify ZIKV and DENV infection in serum and in PBMCs from hospital patients, quantitative real-time RT-PCR was performed. RNA was extracted from 140 μl of serum using the QIAmp Viral RNA Mini kit (Qiagen) and was stored at −80 °C. For PBMCs and monocytes, 50,000-200,000 cells were added to 1 ml of Trizol, RNA was extracted using the PureLink RNA Mini kit (Invitrogen) following the manufacturer’s protocol, and each sample was eluted in 30 μl of nuclease-free water. DNA was removed on column by using 30 U per sample PureLink DNAse (Invitrogen) for 15 min at room temperature. ZIKV RNA in serum was quantified using the ZCD assay with RNA standards[43]. ZIKV RNA in PBMCs was quantified using a modified ZIKV real-time RT-PCR singleplex assay originally developed by the CDC[44]. Primers ZIKV 1086 and ZIKV 1162c were used, with a probe modified to match the Nicaraguan strain Nica 2-16[41] ZIKV_1107-FAM_UG&Nica ([FAM] AGCCTACCTTGACAAGCAGTCAGACACTCAA [BHQ1]). RNA standards consisted of RNA transcripts that were generated from an amplicon derived from ZIKV Nica 2-16

(GenBank KX421194) using the following primer set modified from the CDC singleplex assay[44]: ZIKV 835_T7 ± 10 (5′TAATACGACTCACT ATAGGGAGTCATATACTT GGTCATGATACTGCTGATTGC3′) and ZIKV 1162c ± 10_Nica (5′CAGCCTCTGTCCACTAA CGTTCTTTTGCAGACAT3′). RNA transcripts were generated using RiboMA Large Scale RNA Production System-T7 (Promega). For quantitation, clinical samples and the RNA standards were processed in duplicate on a single run using a Verso 1-Step QRT-PCR Kit (Fisher Scientific). The mean cycle count (Ct) was used for all calculations. The 96-well plate was run on a 7300 Applied Biosystems machine using the following conditions: 50 °C for 30 min, 95 °C for 12.5 min, followed by 40 cycles of 95 °C for 15 s and 60 °C for 1 min. RNA in each sample was quantified by using a linear regression equation for the standard curve, as described previously[45], and the titre was expressed as $\log_{10}$ copies per ml.

TaqMan gene expression assay

RNA (10 μl) from isolated monocytes from ZIKV- or DENV-infected Nicaraguan hospital patients was converted to cDNA using the high-capacity RNA-to-cDNA kit (Applied Biosystems) following the manufacturer's protocol. To determine the relative quantitation of gene expression of chemokines, cytokines and other immune response-related genes, a chemokine TaqMan gene signature plate (Applied Biosystems) was used, containing FAM-(5′) and MGB-(3′) labelled TaqMan probes and corresponding primers for one of the 92 test genes and 4 house-keeping genes as described by the manufacturer (Applied Biosystems). ROX was used as a passive reference dye. For each plate, 1-100 ng cDNA per 20 μl reaction was used, and 10 μl of TaqMan Gene Expression master mix (Applied Biosystems) was added into each well (Applied Biosystems) and run under the following cycling conditions: 50 °C for 2 min, 95 °C for 10 min and then 95 °C for 15 s and 60 °C for 1 min, repeated for 40 cycles using the standard mode on an Applied Biosystems 7300 PCR system. Using the $2^{-\Delta\Delta Ct}$ method, the mRNA-fold change was calculated as previously described, comparing all genes to uninfected monocytes and to the house-keeping gene 18S[46] (Supplementary Fig. 8). Fold changes were visualized by transforming the data to $\log_{10}$ and generating a heatmap using R version 3.3.1.

Statistical analysis

Viraemia and viral load data obtained from cells were analysed using a Mann-Whitney U-test. The flow cytometry data set was analysed using a Student's *t*-test for pairwise comparisons and a one-way analysis of variance (ANOVA) for multiple comparisons applying a Tukey's post-test unless stated otherwise. To calculate statistical differences in outcomes for ZIKV and DENV infection, we used a Pearson's chi-squared test. Statistical significance was defined as $*P < 0.05$, $**P < 0.01$, $***P < 0.001$ and $****P < 0.0001$.

Code availability

The R code for generation of the heatmaps is available from the corresponding author upon request.

Data availability

The data that support the findings of this study are available from the corresponding author upon reasonable request.

Supplementary Material

Refer to Web version on PubMed Central for supplementary material.

Acknowledgments

The authors thank C. Wang for optimizing primers, probes and standards for use of the CDC qRT-PCR assay with Nicaraguan ZIKV strains and J. Waggoner for advice and technical support regarding quantitation of viral RNA using the ZCD qRT-PCR assay. The authors also thank R. Ben-Shachar for help with statistical analysis and graphs, and D. Glasner for his invaluable assistance with figure preparation. Past and present members of the study team based at the Hospital Infantil Manuel de Jesús Rivera, the National Virology Laboratory in the Centro Nacional de Diagnóstico y Referencia of the Nicaraguan Ministry of Health, and the Sustainable Sciences Institute in Managua, Nicaragua, are thanked for their dedication and high-quality work, particularly S. Argüello, W Avilés, C. Cerpas, D. Elizondo, F. McNally, B. Moraga, F. Narváez, A. Núñez, M. de los Ángeles Pérez, M. Vega, R. Zapata and other study personnel. The authors are also grateful to the children who participated in the study and their families. This work was supported by grants U19AI118610 (to E.H.) and R33AI100186 (to A.B. and E.H.) from the National Institute of Allergy and Infectious Diseases, National Institutes of Health (NIH).

References

1. Kuno G, Chang GJJ. Full-length sequencing and genomic characterization of Bagaza, Kedougou and Zika viruses. Arch Virol. 2007; 152:687–696. [PubMed: 17195954]
2. Zika - Epidemiological Update (Americas) (PAHO, 2017). http://www.paho.org/hq/index.php?option=com_docman&task=doc_view&Itemid=270&gid=40222&lang=en
3. D'Ortenzio E, et al. Evidence of sexual transmission of Zika virus. N Engl J Med. 2016; 374:2195–2198. [PubMed: 27074370]
4. Salinas S, Schiavo G, Kremer EJ. A hitchhiker's guide to the nervous system: the complex journey of viruses and toxins. Nat Rev Microbiol. 2010; 8:645–655. [PubMed: 20706281]
5. Garcia-Tapia D, Loiacono CM, Kleiboeker SB. Replication of West Nile virus in equine peripheral blood mononuclear cells. Vet Immunol Immunopathol. 2006; 110:229–244. [PubMed: 16310859]
6. Rios M, et al. Monocytes-macrophages are a potential target in human infection with West Nile virus through blood transfusion. Transfusion. 2006; 46:659–667. [PubMed: 16584445]
7. Durbin AP, et al. Phenotyping of peripheral blood mononuclear cells during acute dengue illness demonstrates infection and increased activation of monocytes in severe cases compared to classic dengue fever. Virology. 2008; 376:429–435. [PubMed: 18452966]
8. Wang WK, et al. Detection of dengue virus replication in peripheral blood mononuclear cells from dengue virus type 2-infected patients by a reverse transcription-real-time PCR assay. J Clin Microbiol. 2002; 40:4472–4478. [PubMed: 12454138]
9. Kou Z, et al. Monocytes, but not T or B cells, are the principal target cells for dengue virus (DV) infection among human peripheral blood mononuclear cells. J Med Virol. 2007; 80:134–146.
10. Ben-Nathan D, Huitinga I, Lustig S, Van Rooijen N, Kobiler D. West Nile virus neuroinvasion and encephalitis induced by macrophage depletion in mice. Arch Virol. 1996; 141:459–469. [PubMed: 8645088]
11. Michlmayr D, Lim JK. Chemokine receptors as important regulators of pathogenesis during arboviral encephalitis. Front Cell Neurosci. 2014; 8:264. [PubMed: 25324719]
12. Faria NR, et al. Establishment and cryptic transmission of Zika virus in Brazil and the Americas. Nature. 2017; 546:406–410. [PubMed: 28538727]
13. Kwissa M, et al. Dengue virus infection induces expansion of a $CD14^{+}CD16^{+}$ monocyte population that stimulates plasmablast differentiation. Cell Host Microbe. 2014; 16:115–127. [PubMed: 24981333]

14. Cros J, et al. Monocytes patrol and sense nucleic acids and viruses via TLR7 and TLR8 receptors. Immunity. 2010; 33:375–386. [PubMed: 20832340]
15. Cerny D, et al. Selective susceptibility of human skin antigen presenting cells to productive dengue virus infection. PLoS Pathog. 2014; 10:e1004548. [PubMed: 25474532]
16. Hamel R, et al. Biology of Zika virus infection in human skin cells. J Virol. 2015; 89:8880–8896. [PubMed: 26085147]
17. Retallack H, et al. Zika virus cell tropism in the developing human brain and inhibition by azithromycin. Proc Natl Acad Sci USA. 2016; 113:14408–14413. [PubMed: 27911847]
18. Richard AS, et al. AXL-dependent infection of human fetal endothelial cells distinguishes Zika virus from other pathogenic flaviviruses. Proc Natl Acad Sci USA. 2017; 114:2024–2029. [PubMed: 28167751]
19. Lemke G. Biology of the TAM receptors. Cold Spring Harb Perspect Biol. 2013; 5:a009076. [PubMed: 24186067]
20. Meertens L, et al. The TIM and TAM families of phosphatidylserine receptors mediate dengue virus entry. Cell Host Microbe. 2012; 12:544–557. [PubMed: 23084921]
21. Peters NC, et al. In vivo imaging reveals an essential role for neutrophils in leishmaniasis transmitted by sand flies. Science. 2008; 321:970–974. [PubMed: 18703742]
22. Ellery PJ, et al. The $CD16^+$ monocyte subset is more permissive to infection and preferentially harbors HIV-1 in vivo. J Immunol. 2007; 178:6581–6589. [PubMed: 17475889]
23. Michlmayr D, et al. Defining the chemokine basis for leukocyte recruitment during viral encephalitis. J Virol. 2014; 88:9553–9567. [PubMed: 24899190]
24. Getts DR, et al. $Ly6c^+$ 'inflammatory monocytes' are microglial precursors recruited in a pathogenic manner in West Nile virus encephalitis. J Exp Med. 2008; 205:2319–2337. [PubMed: 18779347]
25. Faria NR, et al. Zika virus in the Americas: early epidemiological and genetic findings. Science. 2016; 352:345–349. [PubMed: 27013429]
26. Barré-Sinoussi F, Ross AL, Delfraissy JF. Past, present and future: 30 years of HIV research. Nat Rev Microbiol. 2013; 11:877–883. [PubMed: 24162027]
27. Musso D, et al. Potential sexual transmission of Zika virus. Emerg Infect Dis. 2015; 21:359–361. [PubMed: 25625872]
28. Vremec D, et al. Production of interferons by dendritic cells, plasmacytoid cells, natural killer cells, and interferon-producing killer dendritic cells. Blood. 2007; 109:1165–1173. [PubMed: 17038535]
29. Cella M, et al. Plasmacytoid monocytes migrate to inflamed lymph nodes and produce large amounts of type I interferon. Nat Med. 1999; 5:919–923. [PubMed: 10426316]
30. Colonna M, Trinchieri G, Liu YJ. Plasmacytoid dendritic cells in immunity. Nat Immunol. 2004; 5:1219–1226. [PubMed: 15549123]
31. Juffrie M, et al. Inflammatory mediators in dengue virus infection in children: interleukin-8 and its relationship to neutrophil degranulation. Infect Immunol. 2000; 68:702–707. [PubMed: 10639436]
32. Srivastava S, et al. Degradation of Japanese encephalitis virus by neutrophils. Int J Exp Pathol. 1999; 80:17–24. [PubMed: 10365083]
33. Bai F, et al. A paradoxical role for neutrophils in the pathogenesis of West Nile virus. J Infect Dis. 2010; 202:1804–1812. [PubMed: 21050124]
34. Nanki T, Lipsky PE. Cutting edge: stromal cell-derived factor-1 is a costimulator for $CD4^+$ T cell activation. J Immunol. 2000; 164:5010–5014. [PubMed: 10799853]
35. McCandless EE, et al. Pathological expression of CXCL12 at the blood-brain barrier correlates with severity of multiple sclerosis. Am J Pathol. 2008; 172:799–808. [PubMed: 18276777]
36. McCandless EE, Zhang B, Diamond MS, Klein RS. CXCR4 antagonism increases T cell trafficking in the central nervous system and improves survival from West Nile virus encephalitis. Proc Natl Acad Sci USA. 2008; 105:11270. [PubMed: 18678898]
37. Narvaez F, et al. Evaluation of the traditional and revised WHO classifications of dengue disease severity. PLoS Negl Trop Dis. 2011; 5:e1397. [PubMed: 22087348]

38. Waggoner JJ, et al. Viremia and clinical presentation in Nicaraguan patients infected with Zika virus, chikungunya virus, and dengue virus. Clin Infect Dis. 2016; 63:1584–1590. [PubMed: 27578819]
39. Trioplex Real-Time RT-PCR Assay (FDA, 2017). https://www.fda.gov/downloads/medicaldevices/safety/emergencysituations/ucm491592.pdf
40. Zompi S, Montoya M, Pohl MO, Balmaseda A, Harris E. Dominant cross-reactive B cell response during secondary acute dengue virus infection in humans. PLoS Negl Trop Dis. 2012; 6:e1568. [PubMed: 22448292]
41. Tabata T, et al. Zika virus targets different primary human placental cells, suggesting two routes for vertical transmission. Cell Host Microbe. 2016; 20:155–166. [PubMed: 27443522]
42. Balsitis SJ, et al. Tropism of dengue virus in mice and humans defined by viral nonstructural protein 3-specific immunostaining. Am J Trop Med Hyg. 2009; 80:416–424. [PubMed: 19270292]
43. Waggoner JJ, et al. Single-reaction multiplex reverse transcription PCR for detection of zika, chikungunya, and dengue viruses. Emerg Infect Dis. 2016; 22:1295–1297. [PubMed: 27184629]
44. Lanciotti RS, et al. Genetic and serologic properties of Zika virus associated with an epidemic, Yap State, Micronesia, 2007. Emerg Infect Dis. 2008; 14:1232–1239. [PubMed: 18680646]
45. Nolan T, Hands RE, Bustin SA. Quantification of mRNA using real-time RT-PCR. Nat Protoc. 2006; 1:1559–1582. [PubMed: 17406449]
46. Schmittgen TD, Livak KJ. Analyzing real-time PCR data by the comparative CT method. Nat Protoc. 2008; 3:1101–1108. [PubMed: 18546601]

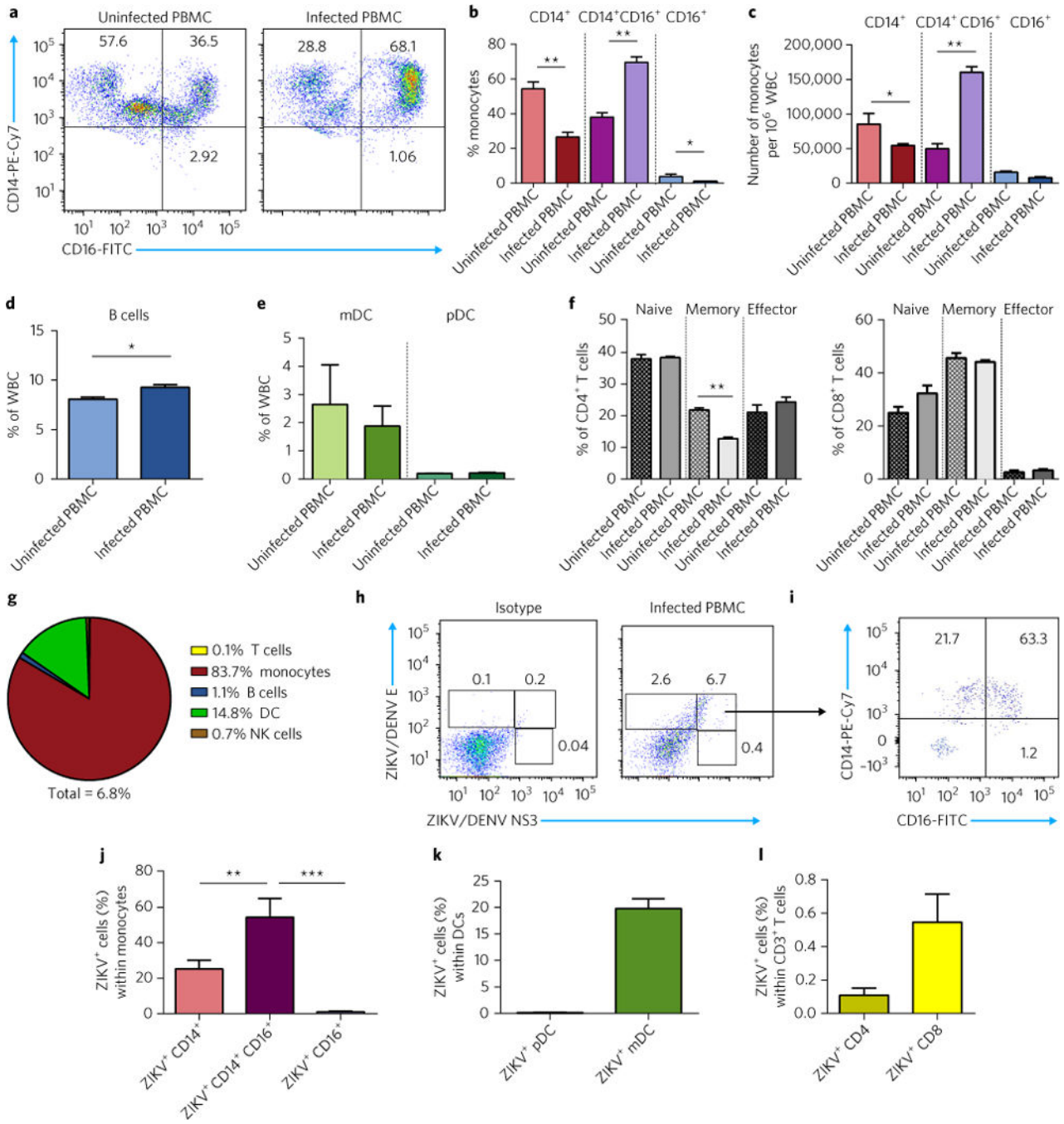

Fig. 1. CD14$^+$CD16$^+$ monocytes are expanded during ZiKV infection compared to uninfected PBMC and are the main target of virus infection in vitro

PBMCs isolated from healthy blood bank donors were infected with ZIKV at an MOI of 1 for 48 h. **a**, Representative dot plots with percentage of CD14$^+$, CD14$^+$CD16$^+$ and CD16$^+$ cells in the monocyte compartment. Cells were pregated on live cells and CD11b$^+$ and HLA-DR$^+$ cells. **b**,**c**, Flow cytometric analysis of the percentage (**b**) and absolute number (**c**) of CD14$^+$, CD14$^+$CD16$^+$ and CD16$^+$ monocytes. **d**,**e**, Frequency of B cells (**d**) and mDCs and pDCs (**e**). **f**, Phenotyping of CD4$^+$ T cells, which were gated on live CD3$^+$ T cells, as

$CD45RA^+CD45RO^-CCR7^+$ naive, $CD3^+CD4^+CD45RA^-CD45RO^+$ memory and $CD3^+CD4^+CD45RA^+$ $CD45RO^-CCR7^-$ effector T cells. **g**, Pie chart showing the mean percentage of cell types within ZIKV-infected (E^+NS3^+) PBMCs. **h**, Representative flow plot of ZIKV-infected (E^+NS3^+) cells within all live WBCs. **i**, Within the E^+ $NS3^+$ cell population, a representative flow plot for ZIKV-infected monocytes. These monocytes were pregated on $CD11b^+HLA\text{-}DR^+$ cells. **j**, Frequency of $CD14^+$, $CD14^+CD16^+$ and $CD16^+$ monocytes that are ZIKV E^+NS3^+. **k**,**l**, Percentage of ZIKV-infected pDCs and mDCs (**k**) or $CD4^+$ and $CD8^+$ T cells (**l**). Mean ± s.d. is shown for all bar graphs. Doublet exclusion was performed for all samples. A representative flow plot for all bar graphs is shown in Supplementary Fig. 1d-j for **d**-**f** and Supplementary Fig. 2a,b for **k** and **l**. Significance was determined by Student's *t*-test or (in **j**) one-way ANOVA with Tukey's post-test. $*P < 0.05$, $**P < 0.01$, $***P < 0.001$. For all panels, $n = 4$ donors from two individual experiments.

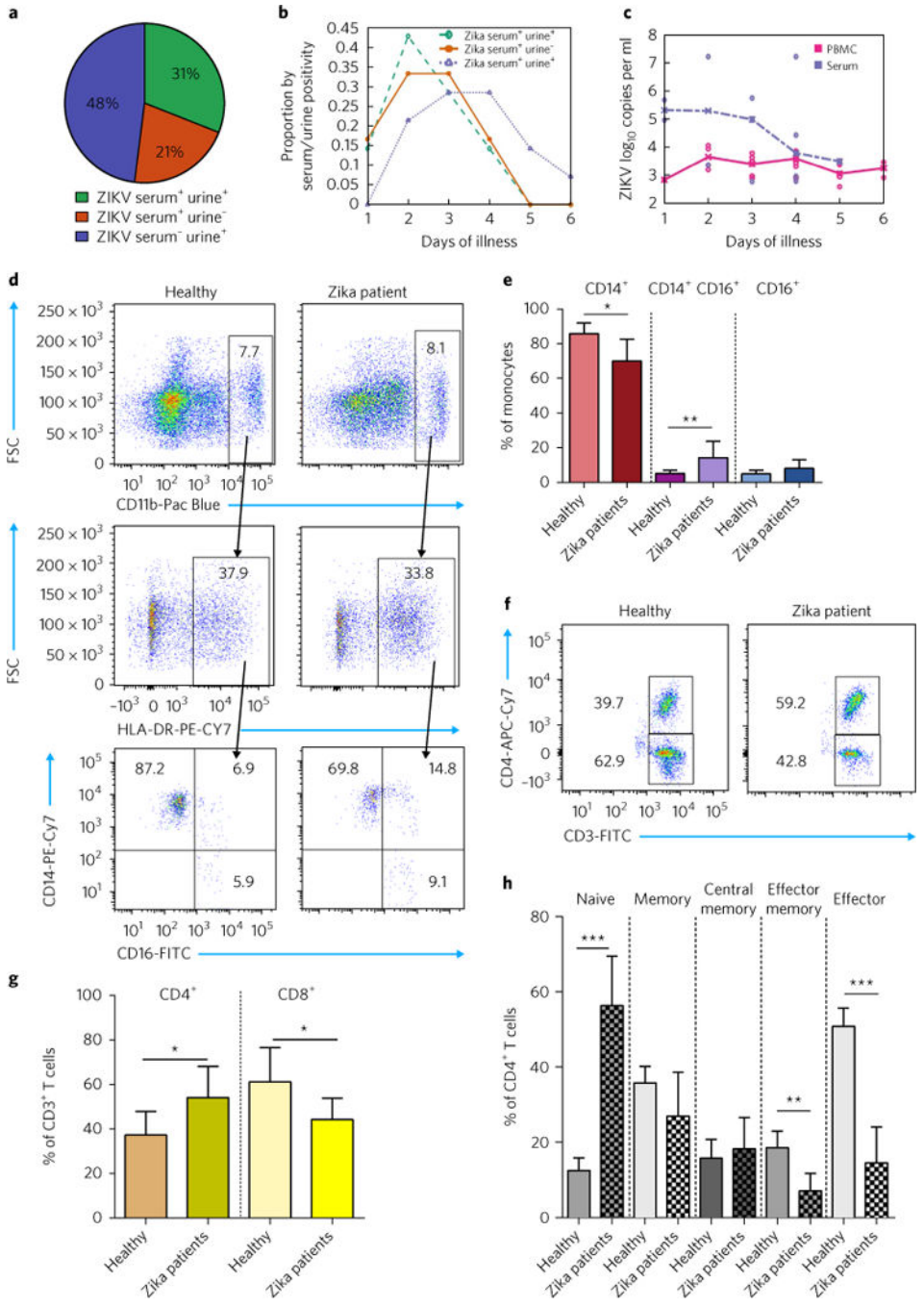

Fig. 2. Detection of ZIKV in serum, PBMCs and urine and characterization of phenotypic changes of cell populations in the blood of Zika patients

a, Frequency of all patients who were ZIKV RT-PCR-positive In serum only (*n* = 6), serum and urine (*n* = 9) or urine only (*n* = 14). **b**, Proportion of serum/urine positivity by day of illness. **c**, Viral titres quantified in PBMCs (*n* = 19) and serum (*n* = 15) by qRT-PCR on day 1 of presentation (days 1-6 post-onset of illness). The median viral titre is shown. In **d**-**h**, phenotypic analyses are shown of changes in cell population in healthy individuals (*n* = 6) and all patients (*n* = 29) that are ZIKV RT-PCR-positive. **d**, Representative dot plots of the

gating strategy used for identifying $CD14^+$, $CD14^+CD16^+$ and $CD16^+$ monocytes within live $CD11b^+$ and HLA-DR^+ cell populations of patients. **e**, Frequency of $CD14^+$, $CD14^+CD16^+$ and $CD16^+$ cells within all monocytes in healthy individuals and Zika cases. **f**, Representative dot plot of $CD4^+$ and $CD8^+$ T cells in a healthy and ZIKV-infected patient. **g**, Frequency of $CD4^+$ and $CD8^+$ T cells within $CD3^+$ T cells. **h**, Phenotypic analysis of $CD4^+$ T cells and identification of naive ($CD45RA^+CD45RO^-CCR7^+$), memory ($CD3^+CD4^+CD45RA^-CD45RO^+$), central memory ($CD3^+CD4^+CD45RA^-CD45RO^+CCR7^-$), effector memory $CD3^+CD4^+CD45RA^-CD45RO^+CCR7^-$) and effector T cells ($CD3^+CD4^+CD45RA^+CD45RO^-CCR7^-$) in healthy and ZIKV-infected individuals. For all bar graphs, mean ± s.d. is shown. Representative flow plots for **h** are provided in Supplementary Fig. 4d. Significance was determined by Student's *t*-test; *P<0.05, **P< 0.01, ***P< 0.001.

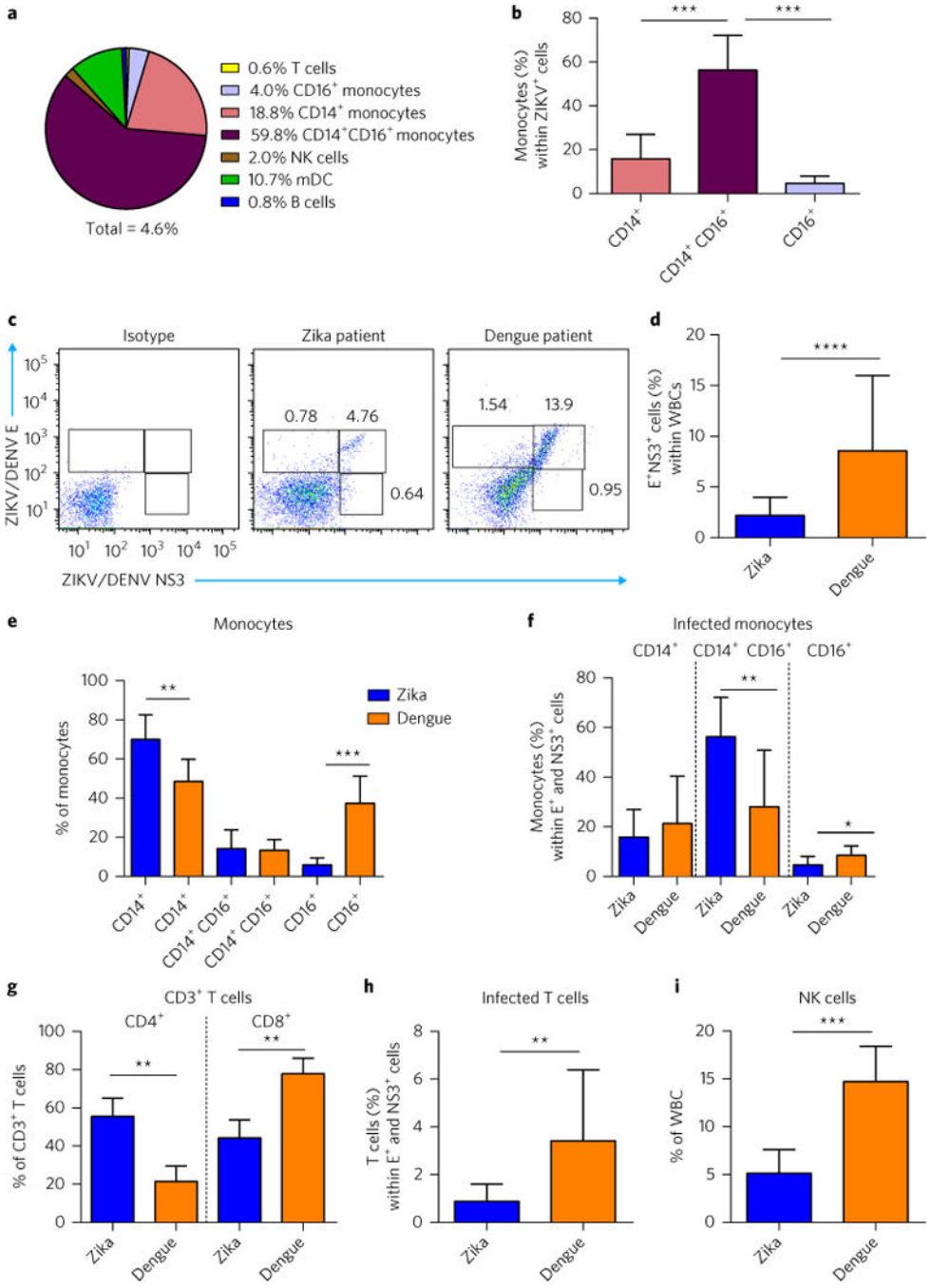

Fig. 3. Staining for ZIKV E and NS3 identifies replicating virus mainly in CD14$^+$CD16$^+$ monocytes in Zika patients, compared to dengue, but viral replication is higher in dengue patients

Infection of WBCs in Zika patients was examined in a subset of Zika patients (n = 19) by staining for E and NS3. **a**, Pie chart showing the mean frequency of cell types that are infected with ZIKV (E$^+$NS3$^+$). **b**, Percentage of CD14$^+$, CD14$^+$CD16$^+$ and CD16$^+$ monocytes that are infected with ZIKV (E$^+$NS3$^+$). Data are from patient samples on day 1 of presentation to the hospital, which is mean day 3.3 post-illness onset (n = 19). In **c**-**i**, infection of WBCs in patients with Zika is compared to WBCs of dengue patients. WBCs

were collected on day 1 of presentation to the hospital from Zika or dengue patients, 3-6 days post-onset of illness. **c**, Representative dot plot of intracellular E and NS3 staining in a ZIKV- and a DENV-infected patient. An isotype control for E and NS3 staining was included. Cells were gated on live PBMCs. Doublet exclusion was performed for all samples. **d**, Percentage of ZIKV or DENV infection (E^+NS3^+) in WBCs from Zika and dengue patients. **e**, Frequency of $CD14^+$, $CD14^+CD16^+$ and $CD16^+$ cells within all monocytes in Zika and dengue patients. **f**, Percentage of infected $CD14^+$, $CD14^+CD16^+$ and $CD16^+$ monocytes (E^+NS3^+) within PBMCs from Zika or dengue cases. **g**, Frequency of $CD4^+$ and $CD8^+$ T cells within $CD3^+$ T cells of ZIKV- or DENV-infected patients. **h**, Staining for E and NS3 within all $CD3^+$ T cells in Zika versus dengue patients. **i**, Frequency of NK cells within PBMCs of ZIKV- or DENV-infected patients. Bar graphs show mean ± s.d.; $n = 19$ (**a**-**d**) or $n = 29$ (**e**, **g**, **i**) Zika patients and $n = 8$ dengue patients. A representative flow plot for **e**-**i** is shown in Supplementary Fig. 6a-d. Significance was determined by Student's *t*-test and, in **b**, one-way ANOVA; *P< 0.05, **P< 0.05, ***P<0.001, ****P<0.0001.

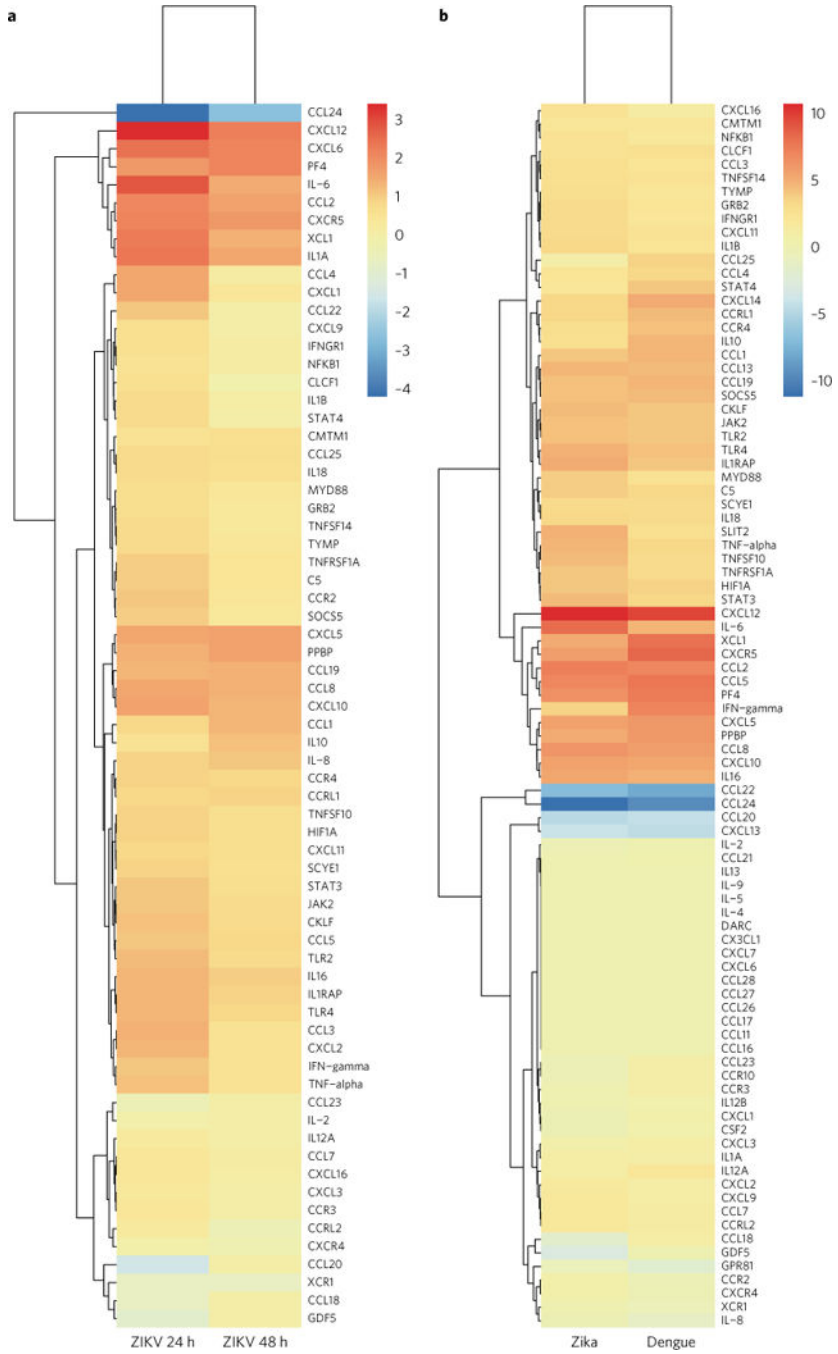

Fig. 4. Gene expression analysis in monocytes from in vitro ZIKV-infected PBMCs or monocytes isolated from Zika and dengue patients reveals significant differences in several cytokines and chemokines

a,b, TaqMan gene expression analysis of in vitro ZIKV-infected monocytes after 24 h or 48 h post-infection at an MOI =1 (**a**) and monocytes isolated from Zika and dengue patients in the acute phase of illness (**b**). Samples were tested in triplicate. Heatmaps are shown for $\log_{10}$-fold changes of mean gene expression. Hierarchical clustering was performed for all

samples using R. $n = 3$ for in vitro ZIKV infection experiments and $n = 3$ each for Zika and dengue patients. Data were derived from two individual experiments.